2014

DOING MORE WITH SHORT PERIOD DATA: DETERMINING MAGNITUDES FROM CLIPPED AND OVER-RUN SEISMIC DATA AT MOUNT ST. HELENS

John J. Wellik II
Michigan Technological University

DOING MORE WITH SHORT PERIOD DATA: DETERMINING MAGNITUDES FROM CLIPPED AND OVER-RUN SEISMIC DATA AT MOUNT ST. HELENS

By

John J. Wellik II

A THESIS

Submitted in partial fulfillment of the requirements for the degree of

MASTER OF SCIENCE

In Geology

MICHIGAN TECHNOLOGICAL UNIVERSITY

2014

This thesis has been approved in partial fulfillment of the requirements for the Degree of MASTER OF SCIENCE in Geology.

Department of Geological and Mining Engineering and Sciences

Thesis Advisor:	*Greg Waite*
Committee Member:	*Simon Carn*
Committee Member:	*Wendy McCausland*
Department Chair:	*John Gierke*

Table of Contents

List of Figures

List of Tables

Semua yang terjadi di bawah kolong langit adalah urusan setiap orang yang berpikir.
Everything under the sun is the business of thinking people.
-Pramoedya Ananta Toer

Preface

All figures and text were prepared by the author. The direction for this work was guided by collaborations with Dr. Greg Waite from Michigan Technological University and Dr. Wendy McCausland from the United States Geological Survey.

Abstract

How can we calculate earthquake magnitudes when the signal is clipped and over-run? When a volcano is very active, the seismic record may saturate (i.e., the full amplitude of the signal is not recorded) or be over-run (i.e., the end of one event is covered by the start of a new event). The duration, and sometimes the amplitude, of an earthquake signal are necessary for determining event magnitudes; thus, it may be impossible to calculate earthquake magnitudes when a volcano is very active. This problem is most likely to occur at volcanoes with limited networks of short period seismometers. This study outlines two methods for calculating earthquake magnitudes when events are clipped and over-run.

The first method entails modeling the shape of earthquake codas as a power law function and extrapolating duration from the decay of the function. The second method draws relations between clipped duration (i.e., the length of time a signal is clipped) and the full duration. These methods allow for magnitudes to be determined within 0.2 to 0.4 units of magnitude. This error is within the range of analyst hand-picks and is within the acceptable limits of uncertainty when quickly quantifying volcanic energy release during volcanic crises. Most importantly, these estimates can be made when data are clipped or over-run.

These methods were developed with data from the initial stages of the 2004-2008 eruption at Mount St. Helens. Mount St. Helens is a well-studied volcano with many instruments placed at varying distances from the vent. This fact makes the 2004-2008 eruption a good place to calibrate and refine methodologies that can be applied to volcanoes with limited networks.

1. Introduction

Effective monitoring during volcanic crises requires quick quantification of geophysical data to interpret activity at the volcano. Analysis need not be made with the precision found in research, but it should reliably represent relative changes in activity as well as describe absolute levels of activity within one order of magnitude. The computational tools used to process the data should be well-tested and simple to use. Finally, the methods should rely on instrumentation that already exists at the volcano.

Many types of data are helpful when monitoring volcanic activity. Gas emissions, heat flux, deformation, seismicity, and aerial imagery all play roles in forecasting eruptive behavior at active volcanoes. Seismometers are the sole monitoring equipment at many volcanoes, thus making seismology a crucial tool during volcanic crises. Seismic monitoring efforts can be limited by the types, quantity, and location of instruments deployed around the volcano.

One critical piece of information that seismologists try to ascertain during volcanic unrest is the total seismic energy release and its rate of increase. Changes in size and type of seismicity during unrest are related to processes such as the volume and rate of magma intrusion or dome growth. Previous research has used cumulative seismic energy release and strain to forecast the timing (Voight 1988, Cruz-Reyna and Reyes-Dávila 2001) and size of eruptions (Prejean and Brodsky 2011). Measuring seismic energy release in pre-eruptive, distal swarms can also be used to determine intrusion volumes underneath volcanoes (White and Power 2001). During a volcanic crisis, observers need to be able to rapidly characterize changes in volcanic activity.

Calculating earthquake magnitudes is a relatively straightforward process during periods of quiescence and moderate unrest. Either the amplitude or the duration of an earthquake seismogram can be used to calculate its magnitude. These magnitudes, in theory, inform about the size of earthquakes generated under the volcano.

Calculating earthquake magnitudes during intense periods of seismic activity is more difficult if the signal is "clipped" or "over-run" (Figure 1). If an earthquake is too large or occurs too close to the seismometer and exceeds the dynamic range of the instrument and digitization equipment, the full amplitude of the signal will not be recorded. In this case, the event is said to be "clipped," "saturated," or "off-scale." When this occurs, it is no longer possible to calculate amplitude-based measurements from the recorded signal. Another problem can occur when events occur close together in time so

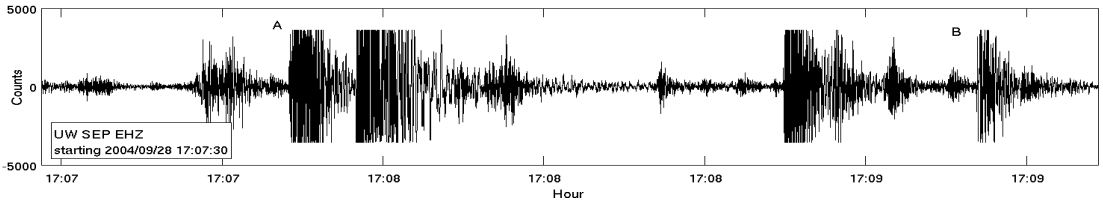

Figure *1.* Examples of clipped and over-run events (A) as well as events that are (B) just clipped.

that the record of one earthquake is not complete before the next one occurs. This means that the duration of the event is not known. If an event is both over-run and clipped, neither a duration magnitude, nor a magnitude based on the amplitude can be calculated.

The purpose of my research is to develop a methodology that can be used to calculate earthquake magnitudes when a signal is clipped, over-run, or both. The method needs to work well for signals that are both severely clipped and over-run. I have developed two methodologies that can be used in combination to calculate earthquake magnitudes when a signal is severely clipped or over-run. The first method was developed by defining the shape of high frequency, volcano tectonic (VT) earthquakes as a power law function and using that function to extrapolate amplitudes and durations from an event. The second method is applicable to severely clipped signals and simply defines a relationship between the "clipped duration" - the amount of time which a signal is clipped - and the full duration of the signal. Magnitudes calculated from my two methodologies are calibrated and compared against picks made by trained analysts to ensure reliability and accuracy.

The procedure of analyzing partial signals to determine event magnitude allows for more reliable quantification of seismic energy release during seismic episodes that are too intense for the installed network. The methodology is designed to be easily transportable from instrument to instrument and network to network. It has direct applicability towards volcanoes with limited networks where quick deployment of additional instrumentation is not a feasible way to get more information during intensifying periods of activity.

2. Background

2.1. Earthquakes and Energy Release

Given a “clean” signal – i.e., a signal that is neither clipped nor over-run – there are a variety of different calculations that can be used for earthquake magnitudes. Two common methods used at volcano observatories are the local magnitude (M_L) and the duration magnitude (M_d).

The local magnitude, sometimes known as the Richter Magnitude, is measured as the peak-to-peak amplitude of the S-wave as measured on a Wood-Anderson seismogram – the type of instrument originally used by Charles Richter (Richter 1935, Gutenberg and Richter 1942). Given the proper instrumentation, local magnitudes have the advantage of being easily calculated and are not compromised by ensuing events. There are several drawbacks, however, in the use of local magnitudes with modern seismic networks. First, the local magnitude formula was empirically derived to be measured on the horizontal component of a Wood-Anderson seismometer. These instruments are no longer in use for practical or scientific seismology purposes. The most common type of instrument used today utilizes a single, vertical component, which may not record the true amplitude of the S-wave. Although IASPEI’s Working Group on Magnitudes (International Association of Seismology and Physics of the Earth’s Interior) does condone the

calculation of local magnitudes using vertical components, accurate measurements require empirical correction factors in addition to those present in the original local magnitude formula (IASPEI 2013). In addition, seismograms must be deconvolved and reconvolved to mimic the response of older instrumentation. This is a straightforward process if instrument response parameters are well-defined, but the response characteristics for instruments at many volcano networks may not be reliably known. Third, the local magnitude formula requires an epicentral distance correction meaning the location of each event should be known. At many volcano networks, it may not be possible to accurately locate all earthquakes due to limitations in the number and placement of available seismometers. Finally, it is impossible to calculate a local magnitude if the earthquake is clipped.

Considering the drawbacks to the local magnitude, duration magnitudes are the preferred magnitude of choice for many volcano monitoring institutions including the Pacific Northwest Seismic Network (PNSN) in the U.S. and the Center for Volcanology and Geologic Hazard Mitigation (CVGHM) in Indonesia. Duration magnitudes, also known as coda magnitudes (M_c), are calculated by measuring the length of time from the P-wave arrival to the point at which the coda drops below the background level (in other words, the end of the event) (Aki and Chouet 1975). This simple approach allows duration magnitudes to be determined with analog paper records or on digital records with no additional computational power. One major advantage of the duration magnitude is that event length does not depend on distance from the source to the station (Aki 1967) up to about 100km (Lee et al. 1972). This means that duration magnitudes can be calculated on any station without epicentral distance factors in most volcano monitoring circumstances. Other advantages to the duration magnitude are that it does not require knowing the instrument response and is not compromised when the signal is clipped.

There are, however, limitations to the utility of duration magnitudes. If an ensuing event occurs before the prior event ends, it is no longer possible to determine the duration of the first event. There are other issues with duration magnitudes related to the source parameters and origin of the coda. Hybrid and low-frequency events, for example, tend to have unusually long codas, and there is debate as to whether or not the coda of these events is related to source properties or scattering (Chouet 1988, Harrington and Brodsky 2007). Because the relationship between duration and magnitude is empirical, however, one could define a unique relation between hybrid and LF coda durations to magnitude assuming source mechanisms were better understood. Despite uncertainty in source property properties of different event types, the same duration magnitude relationship is still relied on heavily for all events for volcano monitoring purposes. Thus, it has been my objective not to provide a means for better determining earthquake magnitudes for different types of events, but rather a methodology for determining magnitudes of any event when it is clipped and over-run.

As an alternative to determining individual earthquake magnitudes, relative measures of seismic activity, such as RSAM and RSEM, are also a simple but valuable way to describe levels and rates of activity at volcanoes. RSAM (Real-time Seismic Amplitude Measurement) and RSEM (Real-time Seismic Energy Measurement) are simple time-window averages of the overall amplitude of a continuous seismic signal

(Figure 2). RSAM and RSEM are valuable tools for volcanic monitoring purposes because they provide quick and easy quantifications of relative seismic energy. RSAM and RSEM also includes contributions of tremor, whereas event-based quantifications do not because there is no magnitude formula for tremor. One drawback to RSAM/RSEM is that the measurements do not discriminate between types of volcanic activity or even natural versus man-made sources. Another limitation of RSAM and RSEM is that it will saturate if all recorded earthquakes are clipped.

Given the utility of both duration magnitudes, RSAM, and RSEM, it is my objective to create a methodology that allows both the amplitude and the duration of the signal to be recovered from partial signals. I do not seek to make judgments on how magnitudes from any derivation should be interpreted but simply to provide a means to acquire the necessary information at intense parts of the seismic signal.

2.2. Volcano Monitoring Networks

The point at which earthquake signals become clipped and over-run is partially dependent on the size and frequency of recorded events. Another factor that affects how soon earthquake signals are clipped and over-run is the network of instruments deployed to monitor seismicity. Well-monitored volcanoes, such as Mount St. Helens, with extensive networks ten seismometers or more installed on or near the flanks of the volcanoes at varying distances and azimuths (Ewert et al. 2005). In essence, the near-by stations can be tuned to record the small, pre-event seismicity while more distal stations can be tuned to record larger events. Monitoring agencies with less extensive networks may not have the luxury of placing and tuning proximal and distal stations for the purpose of recording these phases of seismicity with different stations.

The instrument networks at Mount St. Helens, Sinabung in North Sumatra, and Raung in East Java provide a good example of the range in monitoring networks (Figure 3). During the 2004-2008 eruption, Mount St. Helens had 15 stations installed within 15km of the vent. During its most recent 2013 eruption, Sinabung had 6 stations, while

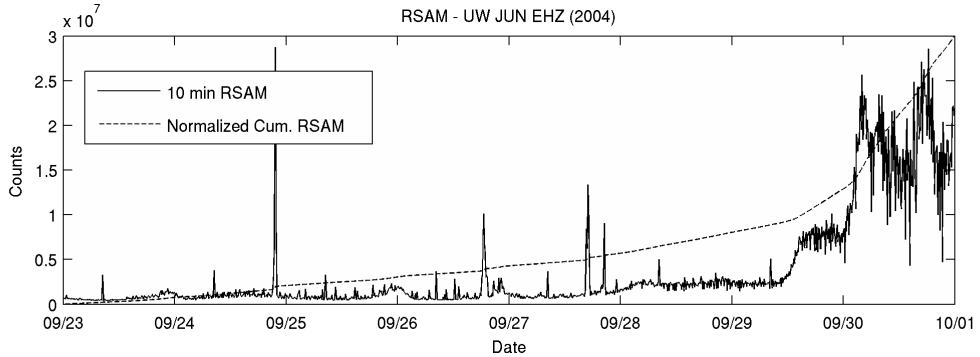

Figure 2. 10 minute RSAM. RSAM displays the average amplitude of the seismic trace over a given time interval. Here, the RSAM at station JUN is displayed for the pre-eruptive stages of the 2004-2008 eruption of Mount St. Helens.

Raung only has 4 stations. Furthermore, the Mount St. Helens network includes broadband sensors, which can be used to study a fuller range of ferquencies, as well as strong-motion sensors that are less prone to clipping.

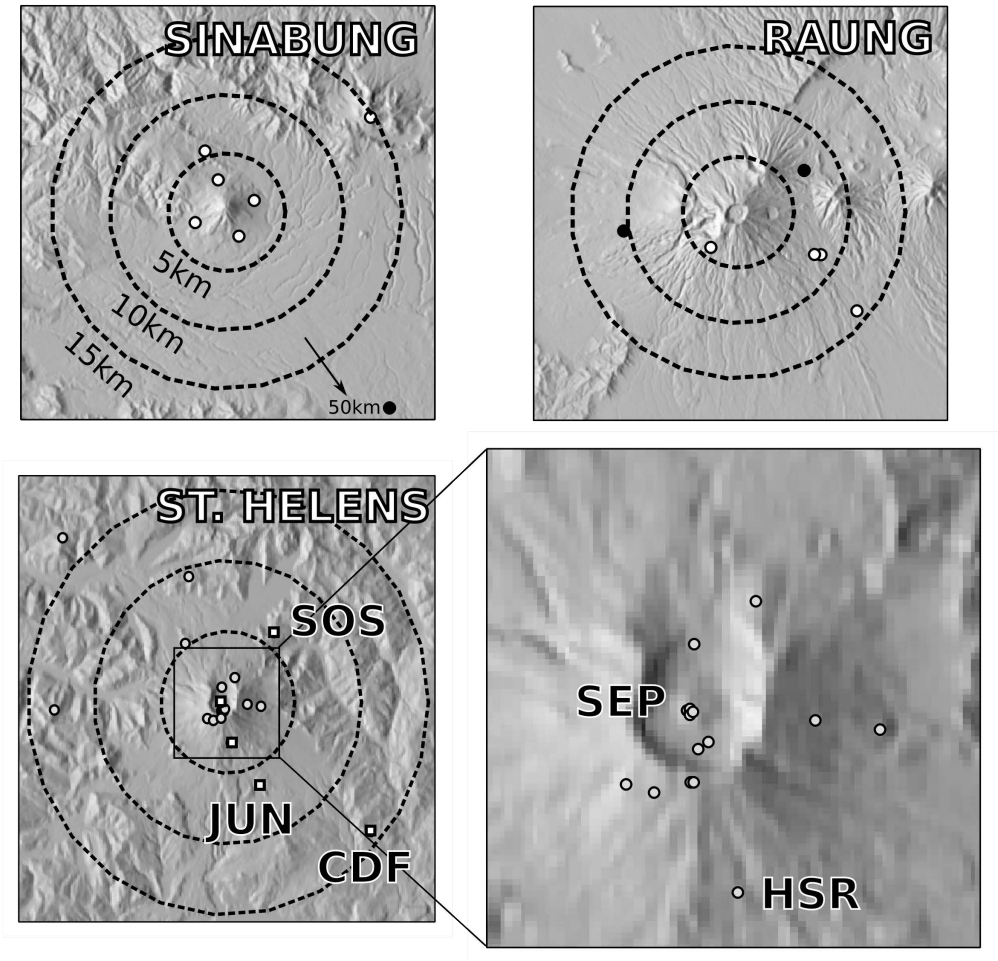

Figure 3. Network maps for three volcanoes illustrating a range of instrumentation. Raung, East Java, Indonesia; Sinabung, North Sumatra, Indonesia; Mount St. Helens, USA. Circles represent short-period vertical stations. Triangles represent short-period three-component stations. Diamonds represent broad-band three component stations. Squares represent strong-motion vertical component instruments.

2.3. Mount St. Helens 2004-2008

After nearly eighteen years of quiescence, a shallow swarm in September 2004 marked the beginning of a new eruptive period at Mount St. Helens. The ongoing eruption included several small explosions and continuous dome growth that lasted through 2008. The seismicity associated with the eruption and the installation of new geophysical instruments, as well as other aspects of the eruption and monitoring efforts, are described in detail by the work published in USGS Professional Paper 1750 (e.g., Horton et al. 2008, Moran et al. 2008a, Moran et al. 2008b, Qamar et al. 2008, Thelen et al. 2008, and McChesney et al. 2008). The detailed account of the volcanic activity and monitoring efforts make this eruption ideal for calibrating and refining a methodology to calculate earthquake magnitudes during periods of unrest.

The 2004-2008 eruption began with the sudden onset of a shallow swarm of volcano-tectonic (VT) earthquakes on 23 September 2004. The early stages of the eruption are split into two temporal categories: the vent clearing phase, which lasted from September 23 to October 5 2004, and the ensuing dome building phase, which started on October 5 2004 and lasted throughout the course of the eruption (Moran et al. 2008a). The Cascades Volcano Observatory (CVO) and the PNSN shared the responsibility of monitoring the volcano's activity in real-time.

This initial phase of activity was marked by relatively low, but persistent seismic activity and several small explosions. The dense seismic network around the volcano (Moran et al. 2008a, McChesney et al. 2008, Thelen et al. 2008), the ability to quickly and safely deploy new instruments near the vent (McChesney et al. 2008), and the development of new monitoring techniques during the eruption (Qamar et al. 2008) allowed the PNSN to locate and calculate magnitudes throughout the eruption. Even then, the large number of rapidly occurring events (over 1 million events were recorded from September 2004 through 2005) caused PNSN to locate and analyze only a representative subset of the data (Thelen et al. 2008) (Figure 4). The large number of highly repetitive events caused PNSN to track relative rates of seismicity with tools such as RSAM and RMS while the cumulative magnitude of the PNSN catalog does not fully quantify the actual seismic energy release during the eruption (Figure 5).

Work done by Moran et al. (2008a) found that the total seismic energy release during this precursory activity was equivalent to a moment magnitude (Mw) 5.5 earthquake, one order of magnitude smaller than the seismic energy release preceding the 1980 May 18 eruption (Md 6.5). Individual event size increased gradually during the vent clearing stage with magnitudes <1.0 to 2.2 during the initial phases with a maximum magnitude of Md 3.9 on October 1 (Moran et al. 2008a).

Following an explosion on October 5, seismicity was dominated by hybrid to low-frequency earthquakes called "drumbeats" for their regular and repeating character (Moran et al. 2008a). Drumbeat event sizes were mostly less than Md 2.0. So called "big" earthquakes (Md > 2.0), associated with migration and growth of the main spine, occurred in four different episodes over the course of the next year and had a cumulative magnitude of Md 4.4 (Moran et al. 2008a).

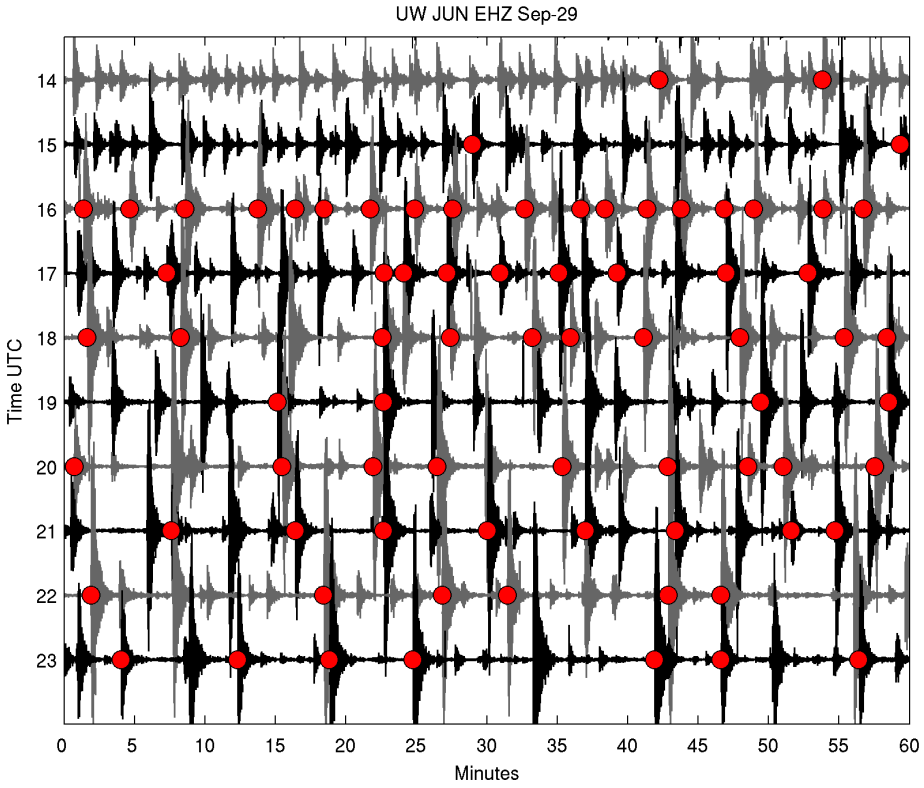

Figure 4. Helicorder showing 10 hours of data from Mount St. Helens in September 2004. Earthquakes occurred so frequently and rapidly during the early stages of seismic activity that PNSN analysts only picked events that were representative of the overall seismicity. Red dots indicate events analyzed for location and duration by the PNSN.

This study considers data from the initial vent-clearing phase from September 23 through September 30. This time period includes the largest concentration of purely VT events that are well recorded as neither clipped nor over-run on stations both near and far from the vent. The seismic activity during the initial phases of the eruption was located in a tight cluster near the surface under the volcano (Thelen et al. 2008) and cover a range of magnitudes consistent with re-awakening volcanoes and dome growth.

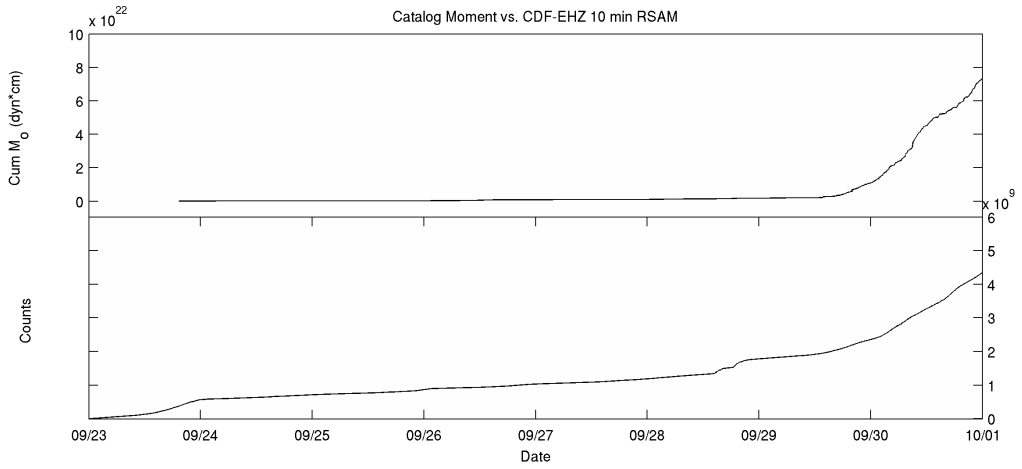

Figure 5. Cumulative energy versus relative RSAM. Catalog energies are summed from the PNSN catalog. RSAM is computed over 10 minute windows at CDF. Overall RSAM increase is more gradual due to small events not being accounted for during the early part of the catalog.

2.4. Relevance to my Peace Corps Service

From April 2011 to June 2013, I lived in East Java, Indonesia as a member of the Peace Corps. Though it may be an unusual inclusion in a geophysics Master's thesis, I would like to take the space to explain the relevance of my two years in East Java to this project. My experience in Indonesia helped shape the direction of my research, and I think it is important for readers of this thesis to understand how the project evolved from the experience.

As a Peace Corps Volunteer in Indonesia, I had two jobs. The first job met the larger objectives of the Peace Corps program in Indonesia while the second job facilitated my work as a Master's student at Michigan Tech. For my “primary project,” I was assigned to teach English at MAN Genteng – a state-sponsored, Islamic secondary school in Genteng, Banyuwangi, East Java. This assignment was personally rewarding in many ways, but providing further details is beyond the purview of this thesis.

For my “secondary project,” I was assigned to work at the Raung volcano observatory in Sragi, Banyuwangi, East Java. The observatory was approximately 30km away from my home and school, and I made the trip weekly by bicycle. Although detailed tasks were not initially delineated for my work at the Raung post, the cooperation was approved by Indonesia's Center for Volcanology and Geologic Hazard Mitigation (CVGHM). Placement at the Raung post was ideal because the United States Geological Survey and U.S. Agency for International Development's Volcano Disaster Assistance Program (USGS-USAID VDAP) had already committed to providing

technical and personnel support at the Raung post and the nearby Ijen post during the two years I was to live in East Java.

The primary tasks of the Raung observatory, while I was present, were to install new seismometers on the volcano and improve analysis capabilities using new computer software. I helped observatory staff choose site locations for new instruments, helped install instruments, helped staff learn new computer software for digital analysis of seismic data, provided background geologic education to staff members, and provided logistical support to visiting members of VDAP.

Despite the addition of new instruments at the volcano, the seismic network around Raung is still quite limited. I learned the limitations of monitoring an active volcano with a small number of short-period instruments at our disposal. I wanted to work on a project that would benefit observers who relied on these type of data, and choose the well-studied and well-instrumented example of Mount St. Helens to develop and refine the methodology.

3. Methodology

In order to consistently project amplitudes and durations of clipped and over-run seismic signals, I modeled the shape of the coda as a simple mathematical function. Past researchers (e.g., Hermann 1975) and the Pacific Northwest Seismic Network (Hartog personal comm., Moran personal comm.) have used a power law function to describe the shape of earthquake codas. Following this lead, I used a select suite of events to empirically derive the power law coefficients that best model high frequency events under Mount St. Helens. Because the shape of an earthquake seismogram is the result of source parameters, site effects, and station response, the model used to define coda envelopes must be site and station specific. Therefore, this process was conducted individually on each station used by PNSN analysts during the vent clearing stage of the 2004-2008 eruption. The accuracy of the model was tested against manually clipped and manually shortened versions of the original data set. The model was then used to extrapolate amplitudes and durations of earthquakes that were actually clipped and over-run during the seismicity of the 2004-2008 eruption. For larger events that are clipped, I compared the length of time that the signal is clipped versus the duration magnitude reported in the PNSN catalog.

3.1. Data Selection – Power Law Model

Developing a methodology to calculate magnitudes for earthquakes that are clipped and over-run requires a suite of seismic signals that are neither clipped nor over-run. The “clean” dataset can be manually clipped and manually over-run to test model estimates against the original data. The clean data set I used to develop my methodology comes from the catalog of events associated with vent-clearing phase of the 2004-2008 eruption of Mount St. Helens. This time period consisted of primarily high frequency VT

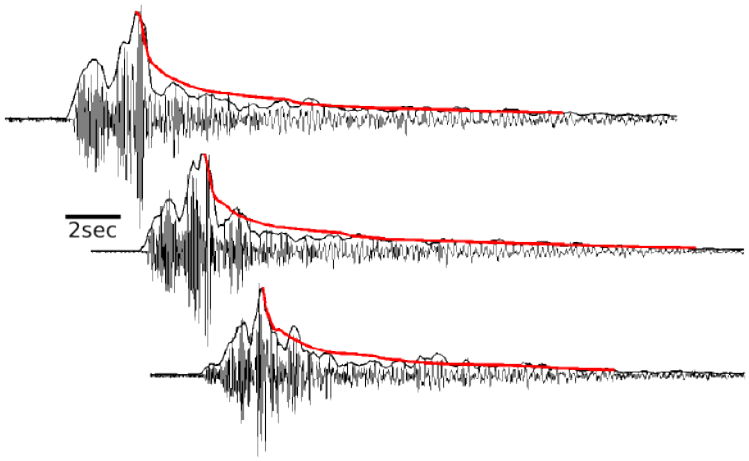

Figure 6. Illustration of the iterative envelope process for three representative events. Solid black line represents the first envelope that can be used to pick phase arrivals. Solid red line represents the re-smoothed coda envelopes. Coda envelopes are compared to power law models.

events located directly underneath the vent at depths of less than 2 km. I used a total of 117 different earthquakes across four different stations for a total of 138 seismograms. The range of averaged catalog magnitudes for these events was Md -1.1 to 1.5.

My first task was to focus on high-frequency earthquakes leading up to the eruption. I choose a representative sample of high-frequency events leading up to the eruption that had already been hand analyzed by PNSN staff. The list of events I used to model coda envelopes at each station is provided in Appendix A.

3.2. Drawing Coda Envelopes

The first step to describing the general shape of high frequency events is to draw the "coda envelope." Drawing coda envelopes is a straight forward process. The intended result is to generalize the shape of the earthquake waveform so that the "envelope" appears similar to how the eye would subjectively determines the signal's shape. I used a two-step process of down sampling and curve smoothing of the seismic signal to produce the coda envelopes (Figure 6).

The first iteration of smoothing is applied to the absolute value trace of the waveform. A moving-average window is applied such that the sample rate is reduced to 10 samples-per-second. The result is a simpler representation of the signal that still shows the P-wave arrival, S-wave arrival, and coda decay. Thus, this envelope can be used to pick phases and durations if onsets are sharp and signal-to-noise ratios are high.

The second iteration of smoothing is only applied to the coda (from the arrival of the S-wave through the duration of the signal). The moving-average window further

simplifies the shape of the earthquake coda but does not further reduce the sample rate. The result is a time-series with one-tenth the original sample rate and a smooth curve that can be reasonably well-represented by a mathematical function.

3.3. Fitting a Mathematical Model

The shape of the coda envelopes are then defined as a power law function. The coda envelope model is defined as

$$f(t)=C*t^{-q}$$

where C is a scaling factor proportional to the absolute maximum amplitude of the signal and q is a constant that controls the rate of the function's decay. The coefficients C and q were empirically defined for each station by finding the best fit power law for each selected coda envelope.

Four stations at varying distance from the Mount St. Helens dome were used to test and calibrate the power law methodology. Only signals that were neither clipped nor over-run and did not possess any other unusual coda characteristics (i.e., “clean” signals) were used for the analysis. Because clipping and over-run signals are more common on stations closer to the earthquake sources, the sample data set of clean signals is smaller for the stations near the vent. Only 10 signals were analyzed on station SEP, 32 on station HSR, 33 on station SOS, and 63 on station JUN. All data used for this study are provided in Appendix A. PNSN analyst duration picks and model estimates for those events are listed in Appendix B.

3.4. Determining Duration from the Power Law Model

The goal of fitting power law models to coda envelope shapes is to describe the initial onset of coda decay. Because power law functions tend to “flatten out” as the time series progresses, it is not always possible to determine when a power law function’s value drops to the background level of the seismic data. Therefore, I chose to determine the end of the event with a mathematical definition. I choose the end of the event at the point where the function’s first derivative rises above -1. This is an arbitrary but easily definable point that yields results consistent with hand-picked durations.

Although defining the end of the coda as a point along the model’s first derivative yields results consistent with hand-picked duration, the results are not the same. When the PNSN started using power law models for earthquake envelopes, the algorithm consistently gave durations about one-half of analyst picks. Therefore, PNSN adjusted their duration magnitude formula accordingly (Table 1).

Table 1.
Duration magnitudes formulas used by PNSN and this study. PNSN formulas are used on all stations in the Cascades regions. Power law modeling in this study requires different formulas for each station. Stations SEP, SOS, and JUN show a trend in increasing y-axis crossing with source-station distance. HSR is known to have unusual coda characteristics and does not follow this pattern.

Duration Magnitude Formulas	
PNSN Pre-2012 - Analyst Hand Picks (Crosson et al. 1972)	
	$Md = -2.46 + 2.82 * \log_{10}(duration)$
PNSN 2012-present – PNSN Power Law Algorithm (Hartog pers. comm.)	
	$Md = -1.61 + 2.82 * \log_{10}(duration)$
Station specific Power Law Formulas - This study	
SEP	$Md = -2.68 + 2.82 * \log_{10}(duration)$
HSR	$Md = -3.09 + 2.82 * \log_{10}(duration)$
SOS	$Md = -2.05 + 2.82 * \log_{10}(duration)$
JUN	$Md = -1.64 + 2.82 * \log_{10}(duration)$

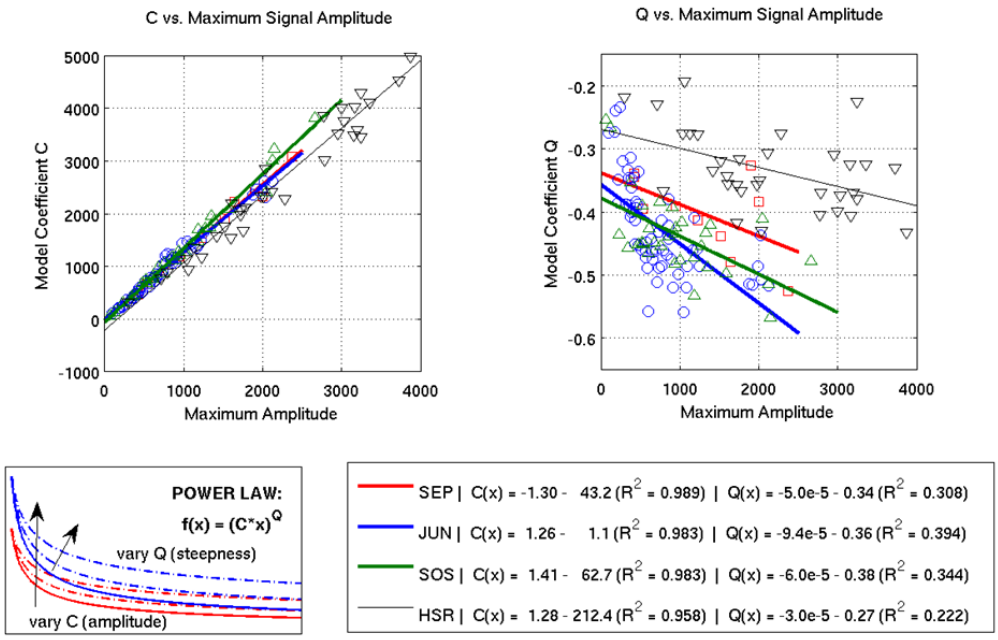

Figure 7. Empirical power law coefficients for four stations surrounding Mount St. Helens. SEP (red squares); JUN (blue circles); SOS (green triangles); HSR (black triangles). Equations for best fit lines are given for coefficient C and coefficient q.

4. Results & Discussion

The steps that were taken to develop the methodologies developed in this study can be presented as a series of questions. How do we describe coda envelopes? How do we fit power law functions to coda envelopes? How do we determine event duration from a power law? How reliable is curve fitting if the event is over-run? Or clipped? What are the limits to which the power laws reliably describe coda envelopes? And - when a power law envelope is not applicable - can we use another measure of duration, such as the clipped duration, to determine magnitude? These were the questions that guided the development of the methodologies put forth in this study. The following section outlines the steps taken to answer each question.

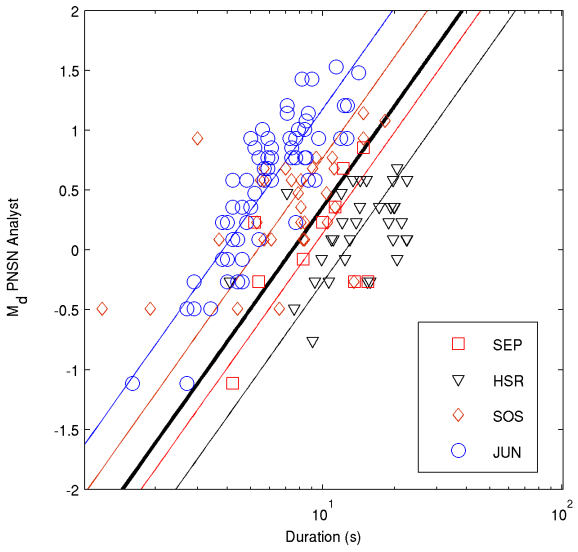

Figure 8 Power law model formulas for stations SEP, HSR, SOS, and JUN. Durations are taken as the point at which the first derivative of the power law model reaches a certain threshold.

4.1. How do we fit power law models to coda envelopes?

Power law models have been used to describe the general shape of tectonic earthquake codas (Hermann 1975) as well as to automatically analyze events in the Cascades range (Moran and Hartog pers. comm. 2014). The first task of this study was to determine how well a power law function fit the shape of high frequency, volcanic earthquakes. Are there consistent relationships between power law coefficients and high frequency earthquake codas from station to station? And if so, what are those coefficients?

Hermann (1975) modeled the shape of tectonic earthquake codas with the equation f(x) = C*t^q where C was a constant scaled with amplitude and q was defined as -1.5. By finding the best fit power law function for a suite of high frequency earthquake codas, the scaling constant and q values were found for four stations situated around Mount St. Helens -- stations SEP, HSR, SOS, and JUN. The amplitude scaling coefficient, C, yielded similar results for each station. Variation in q values, however, were much greater from station to station and did not follow any strong trends with original signal amplitude for any given station. In order to use a power law model to describe earthquake codas, I followed the lead of Hermann (1975) and defined my model with a scaling amplitude factor empirically derived for each station and a fixed value for the exponent, q. These coefficients are provided in Figure 7.

4.2. How do we determine duration from the power law model?

Determining duration from a power law is fundamentally different than the traditional method. Using the traditional method, an analyst hand picks the point at which the coda returns to background noise. Crosson et al. (1972) used this visual method to develop the PNSN's duration magnitude formula given in Table 1. When the PNSN switched from using analyst hand picks to automatic magnitude determination algorithms in 2012, they found that the algorithm consistently gave durations about ½ those picked by analysts, and PNSN adjusted its formula accordingly (Hartog pers. comm. 2014).

Based on the experiences of PNSN, I expected that calculating power law durations would require deriving a new empirical formula to relate duration to magnitude. Ideally, the new equation would be consistent from station to station – a reflection of the fact that coda duration does not scale with source-to-receiver distance.

To achieve this, the PNSN algorithm is based on fitting a power law to the observed data and then assigning a linear fit to a portion of the power law and determining when the linear fit drops below the background noise. This method is only applied to signals that exhibit the full duration of the event – i.e., signals that could be picked by an analyst in the traditional manner.

The purpose of describing the shape of the coda with a power law in this study, however, is to estimate signal duration independent of observations of a return-to-background threshold. Because pre-event background noise levels can fluctuate and increase during episodes of intense seismic unrest, it is also beneficial to be able to estimate duration independent of observations of background noise levels.

For this reason, I choose to define coda duration based on a slope threshold of the power law. After a power law model is fit to the coda, the end of the signal is defined as the point at which the slope of the power law rises above -1. This threshold is arbitrary, but it is chosen to represent a point at which the power law becomes flat.

Defining duration with a slope threshold effectively makes estimated duration a function of power law amplitude. For this reason, station specific correction factors must be introduced to yield similar duration magnitudes for the same event at different stations. This is not an ideal approach because it requires some empirical determinations to be made at each station before the methodology can be used reliably. Nevertheless, the ability to estimate duration (and thus compute a magnitude) based on fitting a power law to part of the coda envelope - even with empirical factors involved - is a useful tool when relying on stations and networks exhibiting clipped and over-run signals. The effectiveness of this method when signals are clipped and over-run is presented in the following sub-sections.

After fitting power law to each earthquake and determining the duration based on the slope of the model, durations were plotted against hand-picked analyst magnitudes (Figure 8). The PNSN formula was then adjusted for each station to yield unique duration

magnitude formulas for each station (Table 1). With the exception of station HSR, the empirical coefficients needed to accurately calculate magnitude on each station scale with distance from source-to-receiver. At stations SEP, SOS, and JUN, there is trend to pick shorter durations with increasing distance. This is a reflection of the fact that amplitude decreases with distance, thus affecting the duration at which a power law function will drop below a static threshold of -1.

Given the empirical constants presented in Table 1, this method provides a reliable estimation of event magnitude. The duration magnitudes estimated made by the model and the analyst-picked duration magnitudes on each individual station are provided in Appendix B. The average difference between model estimates and analyst picks of magnitude across all 138 analyzed signals was 0.3275 magnitude units. Stations SEP, HSR, and JUN all provided reasonable ranges in error while station SOS

4.3. What if the signal is over-run?

The primary purpose of describing coda envelopes with power law functions is to provide a means for estimating durations and magnitudes when signals are clipped and over-run. One important question that needs to be answered, then, is "How well does curve fitting work when a signal is severely over-run?" To test this, I analyzed the best fit between coda envelopes and power law functions at incremental time windows after the S-wave arrival.

Given the coda envelope for an unclipped signal of full duration (i.e., not over-run), I determined the power law that best fit the coda envelope by analyzing the fit at incrementing lengths of time after the S-wave arrival (Figure 9). The algorithm starts by guessing an amplitude of the signal much greater than the station's clip threshold. A power law function corresponding to the guessed amplitude is then created. The guessed power law function is then compared to the actual coda envelope using only the first second of data after the S-wave arrival. Iterative trials are run at decreasing amplitudes down to 50 counts. The amplitude trials are then re-executed using two seconds of data after the S-wave arrival. Successive one-second time windows were analyzed for each signal up to 30 seconds.

Analyzing the power law model at incrementing time windows shows that the best fit power laws are determined with a narrow time band following the S-wave arrival. This supports the intuitive idea that the "steepest" part of the coda decay is the most descriptive characteristic of the coda's shape. Being able to reliably fit a power law curve to a coda by considering only a small amount of time after the S-wave arrival is a powerful tool for determining curve fitting in instances when signals are severely clipped and over-run.

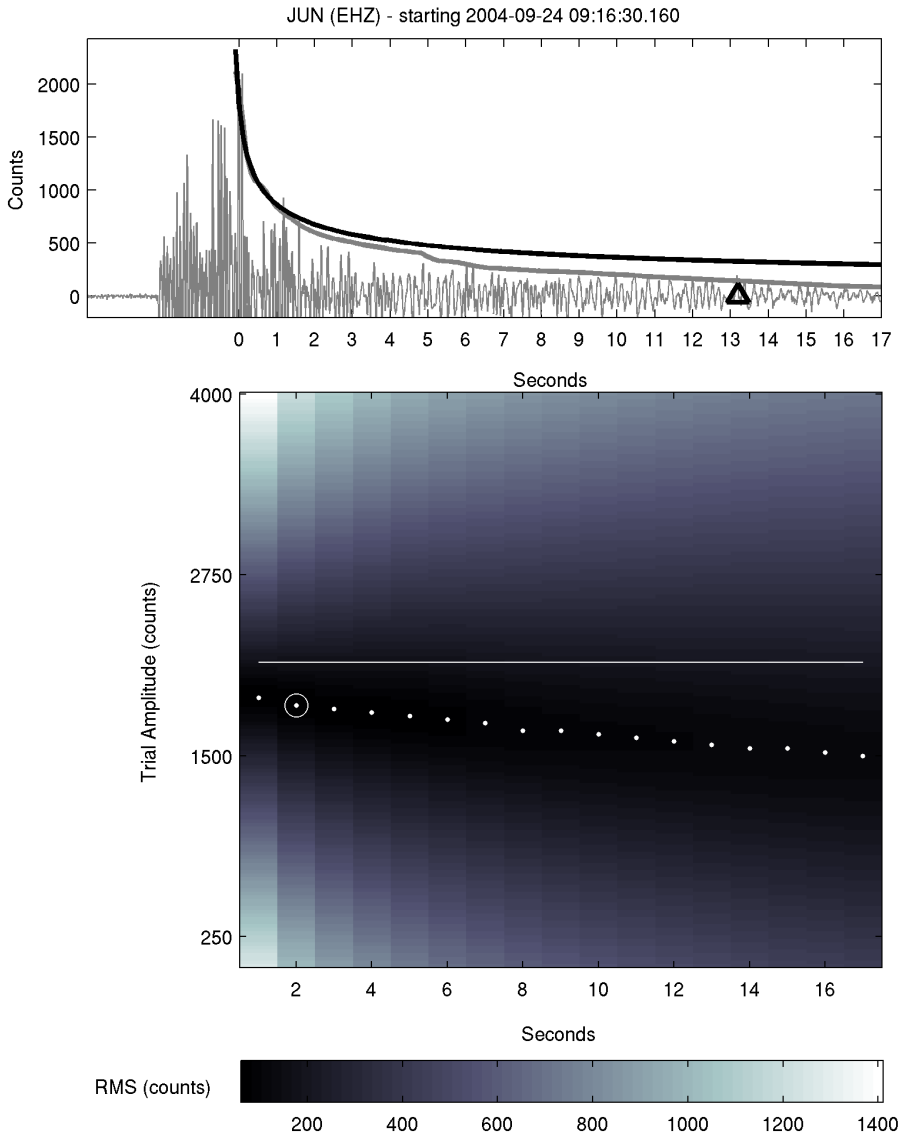

Figure 9. Iterative curve fitting based on incrementing time windows. Power law models (thick black line) were fit to observed coda envelopes (thick grey line) at time windows lengthening by one second. Power laws corresponding to a range of amplitudes were compared to coda envelope dating for each time window. The best estimate of signal amplitude for each time window (white dot) gets progressively poorer – as compared to the signals actual maximum amplitude (white line) – as more time is considered. In this example, the amplitude estimate corresponding to the lowest RMS curve fit (white circle) occurs when considering just two seconds of data after the S-wave arrival.

4.4. What if the signal is clipped?

Another important question that needs to be answered is how well can power law curves be fit if a signal is clipped? If the first few second of the S-wave arrival provide the best fit between power law models and observed coda envelopes, how well can the power law model be fit if the initial part of the signal is missing because it is clipped? To test the performance of curve fitting with clipped data, I manually clipped each signal in the test suite to see how resulting duration and magnitude estimates compared to trials when the signals were not clipped.

I choose two thresholds to clip each signal. The first trial tested curve fitting performance when the signals were clipped at 50% of the original S-wave amplitude arrival, and the second trial used a threshold of 40%. For both thresholds, signals with clipped thresholds of less than 250 counts were not analyzed because of the low signal-to-noise ratio. These thresholds result in signals that are "moderately" clipped. Although 50% and 40% are large percentages of the signal amplitude, only a small amount of time (from less than one to about two seconds) is actually clipped (Figure 10).

Duration and magnitude estimates produced by these tests are provided in Appendix B and Figure 11. Clipping at these thresholds shows little to no variation in duration and magnitude estimates (Figure 11). Intuitively speaking, this shows that it is not just the initial time window after the S-wave arrival that is necessary for fitting power law models but specifically the part of the curve with the greatest curvature. The practical result is that power law curves can be fit to earthquake signals when they are moderately clipped and severely over-run.

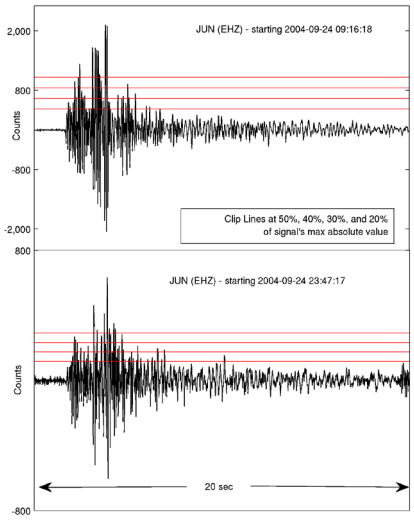

Figure 10. Various clipping thresholds as a percentage of maximum amplitude. Thresholds of 50% and 40% represent "moderate clipping." Thresholds beyond that begin to hide the initial coda shape decay that is crucial for curve fitting.

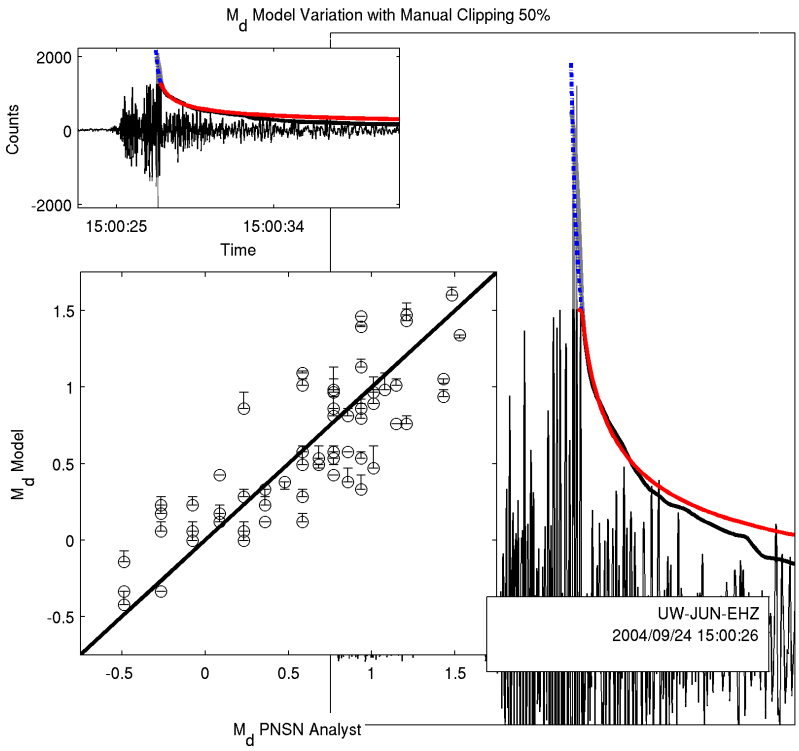

Figure 11. Manually clipped data at 50% of maximum amplitude. Waveform graphic shows the coda envelope and the corresponding best fit power law. The red line represents the portion of the power law used for the curve fitting. The dashed blue line represents the extrapolation of the same power law to the estimated signal amplitude. Plot shows model estimates against PNSN analyst picks with no manual clipping (circles). Error bars represent the change in model estimates for amplitude when the signal is clipped at 50% of the maximum S-wave peak.

4.5. What if the signal is too clipped?

For larger signals that are clipped for longer durations, the steep part of the coda decay is no longer preserved in the earthquake trace. At this point, reliably fitting power law models to the remaining coda envelope is no longer possible. Another method must be used to estimate magnitudes for signals that are over-run. Given consistent and known earthquake locations, the length of time at which a signal is clipped should scale with duration just as full duration scales with magnitude.

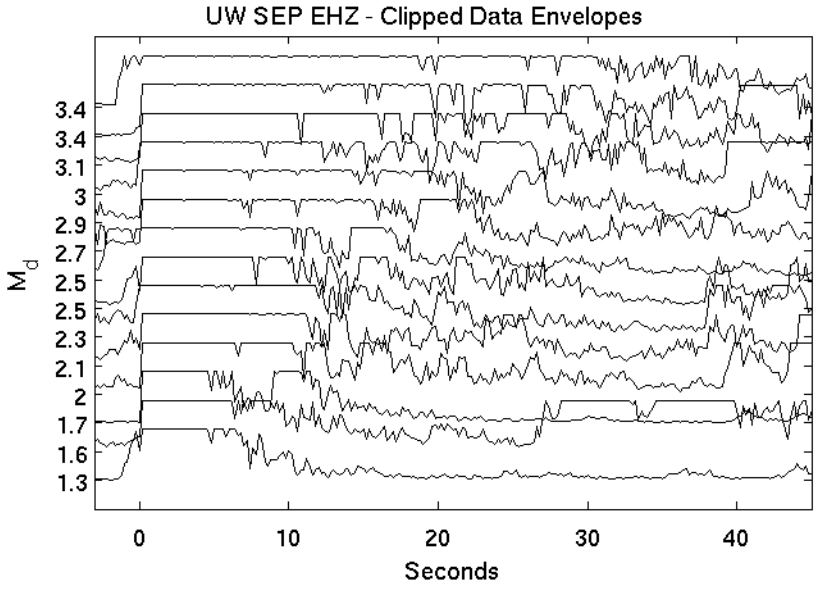

Figure 12. Clipped durations decreasing with magnitude. Smoothed traces of clipped data at station SEP over a range of magnitudes. Reported magnitudes are catalog magnitudes.

4.6. How well does clipped duration mirror full duration magnitude?

As noted previously, the full duration of a signal is the preferred method to compute magnitudes for earthquakes in volcanic settings. The method is advantageous because the duration of an earthquake's signal does not, in theory, vary with distance. The amplitude of the signal, however, does vary with distance. Although signal amplitude decreases with distance from the source, the duration of the signal at its clipped threshold (or any pre-defined amplitude threshold, for that matter) should decrease with magnitude (Figure 12, Figure 13). The equation defining the relationship, however, will vary from station to station instead of remaining fixed as it does for full coda durations.

Given a suite of events with known magnitudes and the same general location, it should be easy to define the relationship between clipped duration and magnitude for each station. Given identical instruments and the same site effects, there should be a trend with decreasing clipped duration and distance from the event.

To show this at Mount St. Helens, I picked clipped durations on four stations at various distances from the vent. Stations SEP (located on the dome), HSR (~4km from the vent), JUN (~6.5km), and CDF (~14km) were all trusted by PNSN analysts to pick full duration magnitudes during the early stages of the 2004 eruption (Moran, pers. comm., 2013). All signals used for this analysis originated from under the vent at depths of 0-2.5km below the surface.

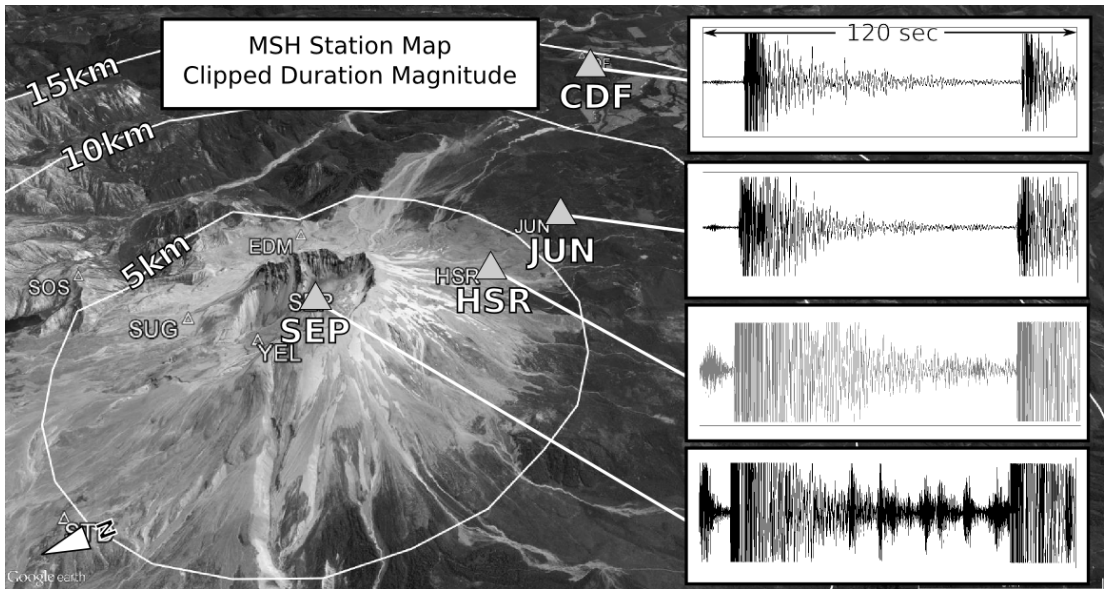

Figure 13. Stations used to determine clipped duration magnitudes. Stations SEP, JUN, and CDF show the expected trend of decreasing clipped duration with distance from the event. Station HSR does not follow this trend. The signal shown on the right is from a Md 3.0 event at 0.83km depth occurring at 2004/09/30 22:12:00 UTC. Aerial imagery from Google, Landsat.

In order to test the suitability of clipped duration magnitude, I measured the clipped duration of large earthquakes registered in the PNSN catalog from September 25 to September 30. Clipped durations on stations SEP, HSR, JUN, and CDF - located <1km, 3.5km, ~6km, and 14km away from the vent, respectively - were compared to catalog magnitudes. The range of magnitudes considered ranged from Md 1.0 to 3.4.

The logarithm of the clipped duration scales linearly with magnitude just as the logarithm of the full duration scales linearly with magnitude. Each station displays a unique static offsets from the PNSN's full duration magnitude formula (Figure 14). These offsets are a result of source-to-station distance, local site effects, and station settings. If local site effects and station settings are held constant, clipped duration should decrease with source-to-station distance. This trend is exhibited with stations SEP, JUN, and CDF. Station HSR tends to have longer ringing codas - likely due to unusual site effects that result in higher amplitudes for longer durations - and does not follow the trend. Although the clipped duration at station HSR does scale log-linearly with catalog magnitude, only a small subset of analyzed signals were able to be used to define the relationship.

Another feature of using clipped duration as a tool for calculating magnitudes is that the lower limit at which it can be used varies from station to station. This is, again, a function of relative signal amplitude as affected by source-to-station distance, local site effects, and station settings. The lower magnitude limit for clipped data at stations SEP and HSR was around Md 1.3, while the lower magnitude limit at stations JUN and CDF was around Md 2.5.

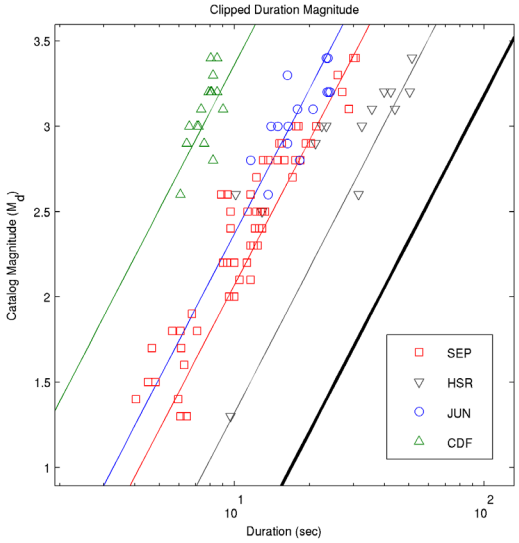

Figure 14. Formula for clipped duration versus PNSN catalog (full duration) magnitudes. Stations SEP, JUN, and CDF show a trend with station distance and y-axis crossing. HSR is an anomaly. See previous figure for station distances. Solid black line represents the equation for the PNSN's (full) duration magnitude formula used at all stations.

5. An application to volcano monitoring

Methodologies for calculating magnitudes with clipped and over-run signals is presented in the sections above. How much can these methodologies affect calculations of total energy release at active volcanoes? To explore the answer to this question, I analyzed data from a twelve hour period of data at Mount St. Helens when seismicity began to increase. I compared the cumulative energy release as tracked by PNSN analysts using the entire network, the cumulative energy release given usable signals at JUN, and the cumulative energy release of a larger number of signals after applying the power law and clipped duration methodologies to the data set (Figure 15)

The PNSN's event database is not meant to be an all-encompassing catalog of events that occurred under the volcano. Rather, the catalog is meant to be representative of the over-all seismicity. Missing from the PNSN's catalog are a large number of over-run small events occurring in rapid succession as well as larger events that have codas over-run by later events.

For the last 12 hours of September 29, the PNSN located and determined magnitudes for 84 total events with a cumulative moment magnitude (Mw) of 3.83. Magnitudes for these events were hand-picked by analysts using the entire network of stations in the Cascades region. Of these 84 events, only 56 have full durations recorded at station JUN located ~7km away from the vent. The cumulative Mw of this smaller suite of events is 3.70, or 40% of the total energy release accounted for in the full catalog.

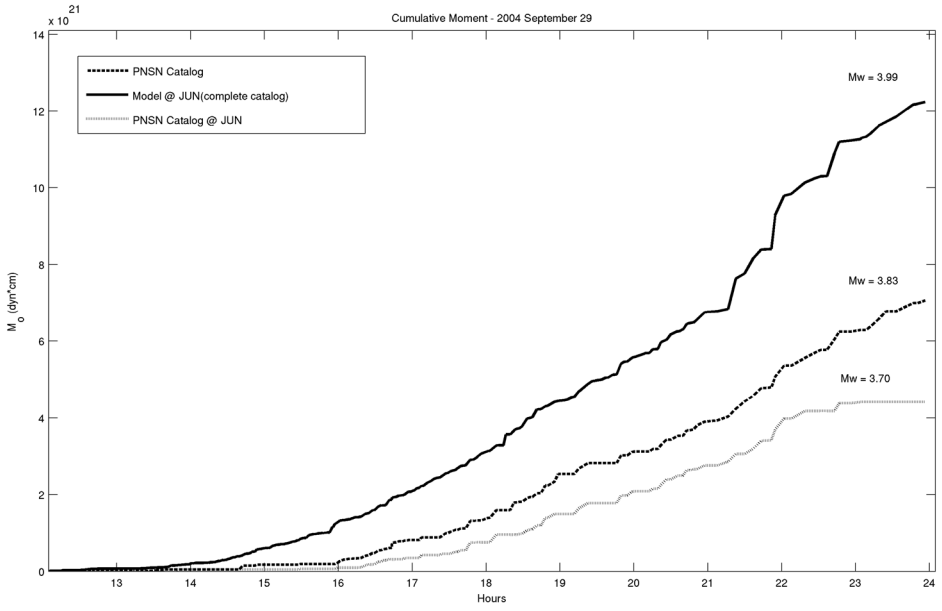

Figure 15. Cumulative energy release as a function of time. Dark dashed line represents 84 events in the PNSN catalog. Light dashed line represents 56 catalog events that can be analyzed on station JUN. Solid black line represents 216 events that can be analyzed with the power law and clipped duration methods on station JUN.

Neither of those moment magnitudes, however, accurately accounts for all seismic energy during this time period. Applying the power law and clipped duration methodologies to the same 12 hours allows magnitudes to be determined for over 250 events using station JUN. The cumulative energy release from JUN using this more complete catalog of events is equivalent to a Mw 3.99. This is 40% more energy than the full PNSN catalog and 100% more than the energy that can be tabulated at JUN using traditional measurements of full duration. The last two hours in this time period exhibit the utility of the power law and clipped duration methods particularly well. During the last two hours on September 29, the traditional method of measuring full duration allows for only 3 events to be cataloged at station JUN. The power law and clipped duration methods, however, allow for 18 events to be accounted for.

6. Conclusions

The ability to continue calculating magnitudes for large events during increasing periods of seismicity is a valuable tool for seismologists and observers monitoring very active volcanoes with limited networks. The appearance of clipped and over-run signals may make this impossible given traditional methods of measuring duration. Fitting a power law to the shape of the coda and extrapolating duration or measuring the clipped duration of the signal, however, are suitable alternatives when data are clipped and over-run.

The empirical calibration factors that must be known for each station can be easily calculated during moderate phases of seismic activity. These calibration factors will remain valid from eruption to eruption assuming station response settings have not been altered and earthquakes are occurring in the same location. For ongoing eruptions, it may be assumed that earthquakes are happening underneath the volcano, and the locations can be treated as consistent. Distal VT swarms, however, may require specific calibration factors to account for varying azimuths and distances from the vent.

Given a reliable and quick software suite for seismic analysis, extrapolating duration using the power law method may be a reliable way for determining magnitudes when it is not otherwise possible. The clipped duration method does not require a computer for analysis and can be used during very intense phases of seismic activity. Both methods reliably estimate magnitudes within error ranges consistent with analyst hand-picks, and both methods could be applied through automatic analysis techniques given computational resources. As with any technique for event analysis, observers and seismologists must apply these methods with proper understanding of station-to-station and site-to-site response that may affect magnitude determinations.

Further investigation still needs to be completed in regards to the performance of the power law method for various types of volcanic earthquakes. High frequency VT events, hybrids, and LF events are all known to have different relationships between signal amplitude and coda duration. The source mechanisms and reasons for this are poorly understood, and thus, it is unclear as to whether the same definition of duration magnitude applies for each event. Just as the full duration methodology is applied to each

of these events, the same parameters and rules for the power law methodology are applied in the same manner to events of various frequency content.

7. Acknowledgments

Many people deserve equal thanks for their efforts in shaping my education – both on campus and abroad. Greg Waite and Wendy McCausland's guidance have made this project enjoyable. Michigan Tech professors Bill Rose, Simon Carn, and John Gierke, alongside Ken Puvak from Peace Corps were instrumental in placing me in Indonesia for my Peace Corps service. My friends and co-workers in Beji, Genteng, and Sragi, East Java all made the experience worthwhile. My fellow Peace Corps Volunteers made it an even richer experience. I would like to thank Pak Surono and Pak Hendra's for allowing me to work with CVGHM staff at the observatories, and I am grateful for the personal and professional relationships I developed with Pak Balok, Pak Bambang, and Pak Mukijo at the Raung post. All of the VDAP staff – Jeff Marso, Andy Lokchart, Rowdy LaFaevers, and Wendy McCauslad – and AVO staff – Matt Haney, John Pastkievich, and Dane Ketner – helped make my experience in East Java an academic one. Once back in the US, the analysis of Mount St. Helens data would not have been possible without the information provided by the PNSN as well as the assistance provided by Seth Moran at CVO and Renate Hartog at PNSN. Double thanks must be given to Mukijo and Wendy for their patience – in both cultural and academic worlds – over the last two and a half years.

8. References

Aki, K. (1967). Scaling law of seismic spectrum. *Journal of Geophysical Research*, *72*(4), 1217–1231. doi:10.1029/JZ072i004p01217

Aki, K., & Chouet, B. (1975). Origin of coda waves: Source, attenuation, and scattering effects. *Journal of Geophysical Research*, *80*(23), 3322–3342. doi:10.1029/JB080i023p03322

Chouet, B. (1988). Resonance of a fluid-driven crack: Radiation properties and implications for the source of long-period events and harmonic tremor. *Journal of Geophysical Research: Solid Earth*, *93*(B5), 4375–4400. doi:10.1029/JB093iB05p04375

Cruz-Reyna, S. D. la, & Reyes-Dávila, G. A. (2001). A model to describe precursory material-failure phenomena: applications to short-term forecasting at Colima volcano, Mexico. *Bulletin of Volcanology*, *63*(5), 297–308. doi:10.1007/s004450100152

Ewert, J.W., Guffanti, M., & Murray T.L. (2005). An Assessment of Volcanic Threat and Monitoring Capabilities in the United States: Framework for a National Volcano Early Warning System. *US Geological Survey Open-File Report 2005-1164.*

Gutenberg, B., & Richter, C. F. (1942). Earthquake magnitude, intensity, energy, and acceleration. *Bulletin of the Seismological Society of America*, *32*(3), 163–191.

Harrington, R. M., & Brodsky, E. E. (2007). Volcanic hybrid earthquakes that are brittle-failure events. *Geophysical Research Letters*, *34*(6), n/a–n/a. doi:10.1029/2006GL028714

Herrmann, R. B. (1975). The use of duration as a measure of seismic moment and magnitude. *Bulletin of the Seismological Society of America*, *65*(4), 899–913.

Horton, S. P., Norris, R. D., & Moran, S. C. (2008). Broadband characteristics of earthquakes recorded during a dome-building eruption at Mount St. Helens, Washington, between October 2004 and May 2005. *US Geological Survey Professional Paper*, (1750), 27–60.

IASPEI. (2013). *Summary of Magnitude Working Group Rrecommendations on Standard Procedures for Determining Earthquake Magnitudes from Digital Data*. Retrieved from http://www.iaspei.org/commissions/CSOI.html#wgmm

Lee, W.H.K., Bennett, R.E., Meagher, K.L. (1972). A Method of Estimating Magnitude of Local Earthquakes from Signal Duration. *US Geological Survey Open File Report*.

McChesney, P. J., Couchman, M. R., Moran, S. C., Lockhart, A. B., Swinford, K. J., & Lahusen, R. G. (2008). Seismic-Monitoring Changes and the Remote Deployment of Seismic Stations (Seismic Spider) at Mount St. Helens, 2004-2005. *US Geological Survey Professional Paper*, (1750), 129–140.

Moran, S. C., Malone, S. D., Qamar, A. I., Thelen, W. A., Wright, A. K., & Caplan-Auerbach, J. (2008a). Seismicity Associated with Renewed Dome Building at Mount St. Helens, 2004-2005. *US Geological Survey Professional Paper*, (1750), 27–60.

Moran, S. C., McChesney, P.J., S. P., & Lockhart, A. B. (2008b). Seismicity and infrasound associated with explosions at Mount St. Helens, 2004-2005. *US Geological Survey Professional Paper*, (1750), 27–60.

Nakahara, H., & Carcolé, E. (2010). Maximum-Likelihood Method for Estimating Coda Q and the Nakagami-m Parameter. *Bulletin of the Seismological Society of America*, *100*(6), 3174–3182. doi:10.1785/0120100030

Nikkilä, M., Polishchuk, V., & Krasnoshchekov, D. (2014). Robust estimation of seismic coda shape. *Geophysical Journal International*, *197*(1), 557–565. doi:10.1093/gji/ggu002

Power, J. A., Coombs, M. L., & Freymueller, J. T. (2010). *The 2006 Eruption of Augustine Volcano, Alaska*. U.S. Geological Survey. Retrieved from http://pubs.usgs.gov/pp/1769/

Prejean, S. G., & Brodsky, E. E. (2011). Volcanic plume height measured by seismic waves based on a mechanical model. *Journal of Geophysical Research: Solid Earth*, *116*(B1), n/a–n/a. doi:10.1029/2010JB007620

Qamar, A. I., Malone, S. D., Moran, S. C., Steele, W. P., & Thelen, W. A. (2008). Near-Real-Time Information Products for Mount St. Helens-Tracking the Ongoing Eruption. *US Geological Survey Professional Paper*, (1750), 61–70.

Richter, Charles F. (1935). An Instrumental Earthquake Magnitude Scale. *Bulletin of the Seismological Society of America*, *25*(1).

Scott, W. E., Sherrod, D. R., & Gardner, C. A. (2008). Overview of the 2004 to 2006, and continuing, eruption of Mount St. Helens, Washington. *US Geological Survey Professional Paper*, (1750), 71–95.

Thelen, W. A., Crosson, R. S., & Creager, K. C. (2008). Absolute and Relative Locations of Earthquakes at Mount St. Helens, Washington, Using Continuous Data: Implications for Magmatic Processes. *US Geological Survey Professional Paper*, (1750), 71–95.

Vallance, J. W., Gardner, C. A., Scott, W. E., Iverson, R. M., & Pierson, T. C. (2010). Mount St. Helens: A 30-Year Legacy of Volcanism. *EOS, Transactions, American Geophysical Union*, *91*(19), 169–170.

Voight, Barry. (1988). A method for prediction of volcanic eruptions. *Nature*, *350*, 695–698. doi:10.1038/350695a0

Appendix A.

Table 2.
Data used to develop power law models. List of signals used to define the shape of coda envelopes for high frequency events at Mount St. Helens. PNSN catalog event times are provided along with the stations used to analyze each signal. PNSN analyst picks and model estimates for the duration of each signal are listed in tables in the text.

ID#	Time UTC	Stations Used
1	23-Sep-2004 02:03:09	SOS
2	23-Sep-2004 11:14:56	SOS
3	23-Sep-2004 12:33:10	SEP
4	23-Sep-2004 13:48:42	SOS, JUN
5	23-Sep-2004 14:35:45	HSR
6	23-Sep-2004 15:05:59	SOS, JUN
7	23-Sep-2004 15:49:56	SOS
8	23-Sep-2004 16:30:55	HSR, SOS
9	23-Sep-2004 17:07:30	HSR
10	23-Sep-2004 17:19:01	HSR
11	23-Sep-2004 17:32:40	JUN
12	23-Sep-2004 17:40:41	SOS, JUN
13	23-Sep-2004 17:59:18	SOS
14	23-Sep-2004 18:27:14	SOS, JUN
15	23-Sep-2004 18:32:33	HSR
16	23-Sep-2004 19:00:38	SOS
17	23-Sep-2004 19:16:50	SOS
18	23-Sep-2004 20:06:02	JUN
19	23-Sep-2004 20:42:57	SEP
20	23-Sep-2004 20:50:35	HSR
21	23-Sep-2004 20:55:19	HSR
22	23-Sep-2004 20:59:41	HSR, SOS
23	23-Sep-2004 21:46:03	HSR
24	23-Sep-2004 21:57:24	JUN
25	23-Sep-2004 22:05:52	HSR
26	23-Sep-2004 22:19:06	SOS

ID#	Time UTC	Stations Used
27	23-Sep-2004 22:49:19	SOS
28	23-Sep-2004 22:56:18	HSR
29	24-Sep-2004 00:00:12	SOS, JUN
30	24-Sep-2004 00:23:09	SOS
31	24-Sep-2004 01:01:54	SEP
32	24-Sep-2004 01:31:59	SOS, JUN
33	24-Sep-2004 01:33:59	SEP
34	24-Sep-2004 01:34:53	SEP
35	24-Sep-2004 01:39:22	SEP
36	24-Sep-2004 01:43:28	SOS
37	24-Sep-2004 01:56:35	SEP
38	24-Sep-2004 01:57:24	HSR
39	24-Sep-2004 02:01:47	HSR
40	24-Sep-2004 02:26:31	SEP
41	24-Sep-2004 02:56:13	SOS, JUN
42	24-Sep-2004 03:56:20	JUN
43	24-Sep-2004 04:02:31	HSR
44	24-Sep-2004 04:21:17	SOS
45	24-Sep-2004 04:27:56	SOS
46	24-Sep-2004 04:40:44	HSR, SOS, JUN
47	24-Sep-2004 04:48:11	HSR, JUN
48	24-Sep-2004 04:59:40	JUN
49	24-Sep-2004 05:25:09	SEP
50	24-Sep-2004 05:36:43	JUN
51	24-Sep-2004 05:51:38	SOS
52	24-Sep-2004 05:59:14	HSR, SOS
53	24-Sep-2004 06:08:11	HSR, JUN
54	24-Sep-2004 06:10:58	JUN
55	24-Sep-2004 06:42:12	JUN
56	24-Sep-2004 07:16:55	HSR
57	24-Sep-2004 07:17:43	JUN
58	24-Sep-2004 07:21:44	JUN
59	24-Sep-2004 07:26:45	SEP

ID#	Time UTC	Stations Used
60	24-Sep-2004 07:47:32	JUN
61	24-Sep-2004 08:07:14	HSR
62	24-Sep-2004 08:20:41	SOS
63	24-Sep-2004 08:23:27	JUN
64	24-Sep-2004 08:31:10	HSR
65	24-Sep-2004 08:35:27	HSR, SOS
66	24-Sep-2004 08:39:17	HSR
67	24-Sep-2004 08:43:27	HSR
68	24-Sep-2004 09:03:42	JUN
69	24-Sep-2004 09:10:40	HSR, JUN
70	24-Sep-2004 09:16:28	JUN
71	24-Sep-2004 10:37:20	JUN
72	24-Sep-2004 10:45:20	HSR
73	24-Sep-2004 10:55:44	JUN
74	24-Sep-2004 11:05:56	JUN
75	24-Sep-2004 11:17:35	JUN
76	24-Sep-2004 11:20:39	JUN
77	24-Sep-2004 11:37:30	JUN
78	24-Sep-2004 11:59:26	SOS
79	24-Sep-2004 12:48:20	JUN
80	24-Sep-2004 13:13:20	JUN
81	24-Sep-2004 13:33:37	HSR
82	24-Sep-2004 14:45:24	JUN
83	24-Sep-2004 14:53:12	JUN
84	24-Sep-2004 15:00:24	JUN
85	24-Sep-2004 15:14:59	JUN
86	24-Sep-2004 15:26:55	JUN
87	24-Sep-2004 15:32:53	JUN
88	24-Sep-2004 15:35:22	JUN
89	24-Sep-2004 16:21:14	JUN
90	24-Sep-2004 16:28:34	JUN
91	24-Sep-2004 16:37:22	SOS, JUN
92	24-Sep-2004 16:41:49	JUN

ID#	Time UTC	Stations Used
93	24-Sep-2004 17:08:49	SOS, JUN
94	24-Sep-2004 18:00:14	JUN
95	24-Sep-2004 18:00:53	JUN
96	24-Sep-2004 18:18:22	JUN
97	24-Sep-2004 18:20:05	JUN
98	24-Sep-2004 18:22:37	JUN
99	24-Sep-2004 18:32:20	JUN
100	24-Sep-2004 19:27:33	JUN
101	24-Sep-2004 20:02:37	JUN
102	24-Sep-2004 20:19:00	HSR, JUN
103	24-Sep-2004 20:24:38	JUN
104	24-Sep-2004 20:57:31	SOS
105	24-Sep-2004 21:01:39	SOS, JUN
106	24-Sep-2004 21:34:41	HSR
107	24-Sep-2004 22:02:20	JUN
108	24-Sep-2004 22:11:46	JUN
109	24-Sep-2004 22:34:31	SOS
110	24-Sep-2004 22:56:12	HSR
111	24-Sep-2004 22:56:58	JUN
112	24-Sep-2004 23:20:19	HSR
113	24-Sep-2004 23:25:56	HSR
114	24-Sep-2004 23:28:11	HSR, JUN
115	24-Sep-2004 23:29:10	JUN
116	24-Sep-2004 23:47:27	JUN
117	24-Sep-2004 23:50:17	JUN

Appendix B.

Table 3.
Power Law Model Results. Comparisons of PNSN analyst picks and power model estimates. PNSN data come from analyst picks on individual stations, not averaged data as is published on online catalogs.

	PNSN Analysts			Model (No Clipping)			Model (50% Clipping)			
ID#	Max Amp. Counts	Dur (s)	MdA	Dur (s)	MdB	Δ1 B-A	Dur (s)	MdC	Δ2 C-A	Δ2 - Δ1
SEP										
3	536	6	-0.27	5.4	-0.61	-0.34	5.6	-0.57	-0.30	0.04
19	423	3	-1.11	4.2	-0.92	0.19	4.4	-0.87	0.24	0.05
31	2367	15	0.86	14.8	0.62	-0.24	15.7	0.69	-0.17	0.07
33	1515	10	0.36	11.3	0.29	-0.07	12.1	0.37	0.01	0.08
34	1898	6	-0.27	15.5	0.68	0.95	16.0	0.72	0.99	0.04
35	1225	9	0.23	10.0	0.14	-0.09	10.7	0.22	-0.01	0.08
37	425	9	0.23	5.2	-0.66	-0.89	5.4	-0.61	-0.84	0.05
40	948	7	-0.08	8.3	-0.09	-0.01	8.9	0.00	0.08	0.09
49	1636	13	0.68	12.2	0.38	-0.30	13.3	0.49	-0.19	0.11
59	2000	6	-0.27	13.6	0.52	0.79	14.3	0.58	0.85	0.06
HSR										
5	293	6	-0.27	4.1	-1.36	-1.09	4.3	-1.30	-1.03	0.06
8	3872	12	0.58	22.5	0.72	0.14	22.5	0.72	0.14	0.00
9	1035	6	-0.27	9.3	-0.36	-0.09	10.6	-0.20	0.07	0.16
10	1758	9	0.23	12.1	-0.04	-0.27	14.4	0.18	-0.05	0.22
15	1121	6	-0.27	10.6	-0.20	0.07	11.6	-0.09	0.18	0.11
20	706	5	-0.49	7.6	-0.61	-0.12	8.8	-0.43	0.06	0.18
21	1057	4	-0.76	9.1	-0.39	0.37	10.6	-0.20	0.56	0.19
22	3723	8	0.09	22.5	0.72	0.63	22.5	0.72	0.63	0.00
23	2117	6	-0.27	15.4	0.26	0.53	17.2	0.39	0.66	0.13
25	1720	8	0.09	13.0	0.05	-0.04	14.7	0.20	0.11	0.15
28	3239	10	0.36	19.3	0.54	0.18	22.5	0.72	0.36	0.18
38	2283	6	-0.27	15.8	0.29	0.56	18.4	0.48	0.75	0.19
39	1419	8	0.09	11.1	-0.14	-0.23	12.4	-0.01	-0.10	0.13
43	1222	7	-0.08	9.9	-0.28	-0.20	11.1	-0.14	-0.06	0.14
46	2998	13	0.68	20.5	0.61	-0.07	22.5	0.72	0.04	0.11
47	1523	7	-0.08	12.4	-0.01	0.07	13.8	0.12	0.20	0.13
52	1596	8	0.09	10.9	-0.16	-0.25	12.5	0.00	-0.09	0.16
53	2788	10	0.36	17.2	0.39	0.03	20.3	0.60	0.24	0.21
56	1721	11	0.48	12.0	-0.05	-0.53	13.4	0.09	-0.39	0.14

	PNSN Analysts			Model (No Clipping)			Model (50% Clipping)			
ID#	Max Amp. Counts	Dur (s)	MdA	Dur (s)	MdB	Δ1 B-A	Dur (s)	MdC	Δ2 C-A	Δ2 - Δ1
61	2016	12	0.58	14.4	0.18	-0.40	17.1	0.39	-0.19	0.21
64	3359	8	0.09	22.4	0.72	0.63	22.5	0.72	0.63	0.00
65	1780	12	0.58	13.4	0.09	-0.49	15.5	0.27	-0.31	0.18
66	3030	10	0.36	19.9	0.57	0.21	22.5	0.72	0.36	0.15
67	3242	9	0.23	21.4	0.66	0.43	22.5	0.72	0.49	0.06
69	1977	10	0.36	14.3	0.17	-0.19	16.5	0.34	-0.02	0.17
72	3198	9	0.23	18.9	0.51	0.28	20.6	0.62	0.39	0.11
81	2955	7	-0.08	20.5	0.61	0.69	22.5	0.72	0.80	0.11
102	3158	8	0.09	19.7	0.56	0.47	21.8	0.68	0.59	0.12
106	1608	9	0.23	13.8	0.12	-0.11	14.9	0.22	-0.01	0.10
110	2038	12	0.58	15.3	0.25	-0.33	16.7	0.36	-0.22	0.11
112	3166	10	0.36	20.0	0.58	0.22	21.9	0.69	0.33	0.11
113	784	11	0.48	7.1	-0.69	-1.17	7.9	-0.56	-1.04	0.13
114	2771	12	0.58	19.7	0.56	-0.02	21.7	0.68	0.10	0.12
SOS										
1	57	5	-0.49	1.2	-1.83	-1.34	1.2	-1.83	-1.34	0.00
2	120	5	-0.49	1.9	-1.26	-0.77	1.9	-1.26	-0.77	0.00
4	853	12	0.58	8.1	0.51	-0.07	8.6	0.59	0.01	0.08
6	1346	14	0.77	11.0	0.89	0.12	11.5	0.94	0.17	0.05
7	1000	11	0.48	7.9	0.48	0.00	8.1	0.51	0.03	0.03
8	761	12	0.58	7.4	0.40	-0.18	7.7	0.45	-0.13	0.05
12	1591	13	0.68	11.2	0.91	0.23	11.6	0.95	0.27	0.04
13	1183	13	0.68	9.1	0.65	-0.03	9.1	0.65	-0.03	0.00
14	522	8	0.09	5.7	0.08	-0.01	5.9	0.12	0.03	0.04
16	606	8	0.09	6.1	0.16	0.07	6.1	0.16	0.07	0.00
17	380	5	-0.49	4.4	-0.24	0.25	4.6	-0.18	0.31	0.06
22	951	8	0.09	8.3	0.54	0.45	8.4	0.56	0.47	0.02
26	595	12	0.58	5.7	0.08	-0.50	5.9	0.12	-0.46	0.04
27	750	5	-0.49	6.6	0.26	0.75	6.6	0.26	0.75	0.00
29	1029	8	0.09	8.4	0.56	0.47	8.6	0.59	0.50	0.03
30	904	9	0.23	8.1	0.51	0.28	8.6	0.59	0.36	0.08
32	1183	14	0.77	9.4	0.69	-0.08	9.6	0.72	-0.05	0.03
36	519	13	0.68	5.7	0.08	-0.60	6.3	0.20	-0.48	0.12
41	936	10	0.36	8.1	0.51	0.15	8.1	0.51	0.15	0.00
44	2151	19	1.15	14.8	1.25	0.10	15.2	1.28	0.13	0.03
45	235	16	0.94	3.0	-0.70	-1.64	3.2	-0.63	-1.57	0.07
46	677	13	0.68	7.0	0.33	-0.35	7.7	0.45	-0.23	0.12

	PNSN Analysts			Model (No Clipping)			Model (50% Clipping)			
ID#	Max Amp. Counts	Dur (s)	MdA	Dur (s)	MdB	Δ1 B-A	Dur (s)	MdC	Δ2 C-A	Δ2 - Δ1
51	941	9	0.23	8.4	0.56	0.33	8.9	0.63	0.40	0.07
52	340	8	0.09	3.7	-0.45	-0.54	4.0	-0.35	-0.44	0.10
62	532	9	0.23	5.3	-0.01	-0.24	5.3	-0.01	-0.24	0.00
65	477	12	0.58	5.5	0.04	-0.54	5.7	0.08	-0.50	0.04
78	2128	16	0.94	14.8	1.25	0.31	15.3	1.29	0.35	0.04
91	2046	6	-0.27	13.5	1.14	1.41	13.9	1.17	1.44	0.03
93	2663	18	1.08	18.2	1.50	0.42	20.2	1.63	0.55	0.13
104	1379	10	0.36	11.3	0.92	0.56	11.9	0.98	0.62	0.06
105	1277	11	0.48	10.4	0.82	0.34	10.9	0.88	0.40	0.06
109	1324	9	0.23	10.5	0.83	0.60	11.2	0.91	0.68	0.08
JUN										
4	840	15	0.90	7.4	0.80	-0.10	7.7	0.86	-0.04	0.06
6	1254	16	0.90	9.6	1.10	0.20	10.0	1.18	0.28	0.08
11	93	3	-1.10	1.6	-1.10	0.00	1.6	-1.06	0.04	0.04
12	1156	18	1.10	8.5	1.00	-0.10	9.3	1.09	-0.01	0.09
14	433	10	0.40	4.6	0.20	-0.20	4.8	0.28	-0.12	0.08
18	220	3	-1.10	2.7	-0.40	0.70	2.7	-0.42	0.68	-0.02
24	351	9	0.20	4.0	0.10	-0.10	4.2	0.12	-0.08	0.02
29	854	9	0.20	7.7	0.90	0.70	8.4	0.97	0.77	0.07
32	771	20	1.20	7.1	0.80	-0.40	7.4	0.81	-0.39	0.01
41	571	10	0.40	5.0	0.30	-0.10	4.8	0.28	-0.12	-0.02
42	586	14	0.80	5.4	0.40	-0.40	5.4	0.43	-0.37	0.03
46	446	16	0.90	5.0	0.30	-0.60	5.4	0.43	-0.47	0.13
47	186	5	-0.50	2.9	-0.30	0.20	2.9	-0.34	0.16	-0.04
48	425	6	-0.30	4.6	0.20	0.50	4.8	0.28	0.58	0.08
50	570	15	0.90	5.2	0.40	-0.50	5.6	0.47	-0.43	0.07
53	427	12	0.60	4.8	0.30	-0.30	5.0	0.33	-0.27	0.03
54	1925	20	1.20	12.3	1.40	0.20	13.1	1.51	0.31	0.11
55	479	10	0.40	4.2	0.10	-0.30	4.2	0.12	-0.28	0.02
57	791	17	1.00	8.4	1.00	0.00	9.1	1.06	0.06	0.06
58	646	12	0.60	6.1	0.60	0.00	6.3	0.61	0.01	0.01
60	734	14	0.80	6.1	0.60	-0.20	6.3	0.61	-0.19	0.01
63	360	7	-0.10	3.8	0.00	0.10	4.0	0.06	0.16	0.06
68	913	14	0.80	7.4	0.80	0.00	7.7	0.86	0.06	0.06
69	375	12	0.60	4.2	0.10	-0.50	4.4	0.17	-0.43	0.07
70	2120	20	1.20	12.7	1.50	0.30	13.5	1.55	0.35	0.05
71	657	14	0.80	5.9	0.50	-0.30	5.7	0.49	-0.31	-0.01

	PNSN Analysts			Model (No Clipping)			Model (50% Clipping)			
ID#	Max Amp. Counts	Dur (s)	MdA	Dur (s)	MdB	Δ1 B-A	Dur (s)	MdC	Δ2 C-A	Δ2 - Δ1
73	773	14	0.80	8.5	1.00	0.20	9.6	1.13	0.33	0.13
74	270	7	-0.10	4.0	0.10	0.20	4.2	0.12	0.22	0.02
75	687	13	0.70	5.9	0.50	-0.20	6.3	0.61	-0.09	0.11
76	1096	12	0.60	8.7	1.00	0.40	9.0	1.05	0.45	0.05
77	1881	16	0.90	11.9	1.40	0.50	12.0	1.40	0.50	0.00
79	656	13	0.70	5.7	0.50	-0.20	5.6	0.47	-0.23	-0.03
80	2025	25	1.50	14.1	1.60	0.10	14.7	1.65	0.15	0.05
82	894	19	1.10	7.1	0.80	-0.30	7.1	0.76	-0.34	-0.04
83	389	6	-0.30	4.4	0.20	0.50	4.6	0.23	0.53	0.03
84	1992	16	0.90	12.6	1.50	0.60	12.6	1.46	0.56	-0.04
85	390	8	0.10	4.2	0.10	0.00	4.4	0.17	0.07	0.07
86	347	6	-0.30	4.0	0.10	0.40	4.2	0.12	0.42	0.02
87	849	14	0.80	7.7	0.90	0.10	8.2	0.94	0.14	0.04
88	238	9	0.20	3.8	0.00	-0.20	4.0	0.06	-0.14	0.06
89	177	6	-0.30	2.9	-0.30	0.00	2.9	-0.34	-0.04	-0.04
90	465	8	0.10	4.4	0.20	0.10	4.6	0.23	0.13	0.03
91	862	17	1.00	7.9	0.90	-0.10	8.5	0.98	-0.02	0.08
92	1179	12	0.60	9.3	1.10	0.50	9.4	1.10	0.50	0.00
93	2030	26	1.50	11.4	1.30	-0.20	11.2	1.32	-0.18	0.02
94	639	8	0.10	5.4	0.40	0.30	5.4	0.43	0.33	0.03
95	478	12	0.60	5.7	0.50	-0.10	6.1	0.57	-0.03	0.07
96	441	9	0.20	4.8	0.30	0.10	5.0	0.33	0.13	0.03
97	317	5	-0.50	3.4	-0.10	0.40	3.6	-0.07	0.43	0.03
98	412	8	0.10	4.2	0.10	0.00	4.4	0.17	0.07	0.07
99	729	16	0.90	7.3	0.80	-0.10	7.9	0.89	-0.01	0.09
100	389	6	-0.30	4.0	0.10	0.40	4.0	0.06	0.36	-0.04
101	219	5	-0.50	2.7	-0.40	0.10	2.9	-0.34	0.16	0.06
102	856	14	0.80	8.4	1.00	0.20	9.0	1.05	0.25	0.05
103	372	7	-0.10	4.6	0.20	0.30	4.8	0.28	0.38	0.08
105	1085	16	0.90	7.7	0.90	0.00	8.1	0.92	0.02	0.02
107	707	15	0.90	6.1	0.60	-0.30	6.1	0.57	-0.33	-0.03
108	975	19	1.10	8.7	1.00	-0.10	9.0	1.05	-0.05	0.05
111	1218	24	1.40	9.0	1.10	-0.30	8.8	1.02	-0.38	-0.08
114	514	17	1.00	5.6	0.50	-0.50	6.3	0.61	-0.39	0.11
115	1052	24	1.40	8.2	0.90	-0.50	8.5	0.98	-0.42	0.08
116	580	16	0.90	5.9	0.50	-0.40	6.1	0.57	-0.33	0.07
117	596	11	0.50	5.2	0.40	-0.10	5.0	0.33	-0.17	-0.07

Appendix C.

Table 4.
Clipped Duration Data. A list of signals located under Mount St. Helens used to calibrate a methodology for calculating "clipped duration" magnitudes at stations SEP, HSR, JUN, and CDF. Reported magnitudes are averaged catalog magnitudes.

Time UTC	Md	Time UTC	Md
2004/09/23 19:20:06	2.7	2004/09/25 04:12:39	1.6
2004/09/24 01:07:53	1.3	2004/09/25 04:14:59	1.2
2004/09/24 01:31:59	1.0	2004/09/25 04:19:42	1.5
2004/09/24 02:55:34	1.1	2004/09/25 04:51:37	1.2
2004/09/24 03:08:03	1.4	2004/09/27 21:25:04	1.8
2004/09/24 03:33:02	2.2	2004/09/27 21:40:12	1.7
2004/09/24 04:27:56	1.0	2004/09/27 22:08:52	1.5
2004/09/24 08:12:27	1.3	2004/09/27 22:22:30	1.3
2004/09/24 09:16:28	1.6	2004/09/27 23:03:21	1.2
2004/09/24 10:26:14	1.0	2004/09/27 23:25:36	1.4
2004/09/24 11:59:26	1.3	2004/09/27 23:46:21	1.5
2004/09/24 12:04:54	1.5	2004/09/27 23:53:21	1.8
2004/09/24 13:13:20	1.2	2004/09/29 13:33:49	2.0
2004/09/24 14:04:25	1.4	2004/09/29 13:38:31	1.4
2004/09/24 17:08:49	1.4	2004/09/29 13:50:46	3.1
2004/09/24 18:04:46	1.0	2004/09/29 14:42:13	2.6
2004/09/24 19:19:06	1.7	2004/09/29 14:53:48	2.2
2004/09/24 22:11:46	1.1	2004/09/29 15:28:57	2.0
2004/09/24 22:41:45	1.0	2004/09/29 15:59:18	2.3
2004/09/24 22:42:14	1.1	2004/09/29 16:01:21	2.4
2004/09/24 22:56:58	1.3	2004/09/29 16:04:37	2.3
2004/09/24 23:29:10	1.2	2004/09/29 16:08:34	2.1
2004/09/24 23:47:27	1.0	2004/09/29 16:13:42	2.0
2004/09/24 23:52:09	1.0	2004/09/29 16:16:23	1.6
2004/09/24 23:57:52	1.4	2004/09/29 16:18:27	1.9
2004/09/25 01:06:12	1.1	2004/09/29 16:21:42	2.4
2004/09/25 02:31:43	1.4	2004/09/29 16:24:52	2.2

Continued on next page…

...Continued from previous page

Time UTC	Md	Time UTC	Md
2004/09/29 16:27:34	2.4	2004/09/29 22:42:52	2.9
2004/09/29 16:32:40	2.5	2004/09/29 22:46:36	2.8
2004/09/29 16:36:38	2.3	2004/09/29 23:04:00	2.3
2004/09/29 16:38:22	1.5	2004/09/29 23:12:17	2.6
2004/09/29 16:41:20	2.2	2004/09/29 23:18:49	2.8
2004/09/29 16:43:46	2.7	2004/09/29 23:24:44	2.8
2004/09/29 16:46:50	1.8	2004/09/29 23:41:53	2.7
2004/09/29 16:48:56	2.2	2004/09/29 23:46:36	2.5
2004/09/29 16:53:50	2.2	2004/09/29 23:56:23	2.5
2004/09/29 16:56:42	1.8	2004/09/30 21:07:31	3.1
2004/09/29 17:07:15	2.5	2004/09/30 21:30:29	3.4
2004/09/29 17:22:41	1.7	2004/09/30 21:37:25	3.2
2004/09/29 17:24:04	2.3	2004/09/30 21:46:16	2.6
2004/09/29 17:27:09	2.5	2004/09/30 21:57:55	3.4
2004/09/29 17:30:54	2.3	2004/09/30 22:12:00	3.0
2004/09/29 17:35:05	2.4	2004/09/30 22:22:29	3.3
2004/09/29 21:07:36	2.3	2004/09/30 22:28:50	3.2
2004/09/29 21:16:23	2.6	2004/09/30 22:34:55	3.0
2004/09/29 21:22:39	2.8	2004/09/30 22:44:04	3.1
2004/09/29 21:30:02	2.8	2004/09/30 22:47:34	2.9
2004/09/29 21:36:57	2.7	2004/09/30 23:05:37	2.9
2004/09/29 21:43:21	2.8	2004/09/30 23:09:24	3.2
2004/09/29 21:51:34	2.1	2004/09/30 23:16:39	1.3
2004/09/29 21:54:41	2.9	2004/09/30 23:34:12	3.2
2004/09/29 22:01:53	2.9	2004/09/30 23:39:22	2.6
2004/09/29 22:18:25	2.8	2004/09/30 23:50:45	3.0
2004/09/29 22:26:48	2.7	2004/09/30 23:53:26	2.5
2004/09/29 22:31:26	2.5	2004/09/30 23:55:50	2.8